Light-induced current in plasma

S. N. Atutov, K. A. Nasyrov, S. P. Pod'yachev, A. M. Shalagin, and O. A. Vostrikov
Institute of Automation and Electrometry, Novosibirsk 630090, Russia
(Received 5 February 1996)

The theory of light-induced current (LIC) in plasma, and the results of experimental investigation of this effect are presented. The current was induced by laser radiation in helium and hydrogen rf discharge. The measured magnitude of this current was 1 μA in helium and 0.04 μA in hydrogen plasma. The theoretical estimations of LIC magnitude, its dependence on laser frequency detuning, and gas pressure are found to be in good agreement with experimental data. The application of LIC in measuring ionization and transport collision rates of excited atoms is also discussed. A light-induced current may have been an important mechanism in the magnetic field generation in stellar atmospheres, in particular, in the solar atmosphere. [S1050-2947(96)09410-3]

PACS number(s): 42.50.Vk, 34.50.Gb, 32.80.Rm, 82.80.Kq

I. INTRODUCTION

Light-induced gas-kinetic phenomena have been the subject of intense investigation for the past 15 years [1–4]. The common feature of these phenomena is the velocity-selective optical excitation of the absorbers. The flux of excited particles has properties which are different from those of the flux of nonexcited particles because of a larger cross-section for interaction with the surrounding gas. For example, a difference in the transport collision rate of excited and nonexcited particles with buffer gas particles leads to pulling or pushing of the absorbers in a laser beam [2] or to light-induced drift of the absorbers [1] (and therefore to electrical current if the absorbers are ions [3]). The electrical current may also be induced in initially neutral gas if the velocity-selective excited particles have a higher probability to react with other atoms accomplished by ionization [5,6].

Recently the interest in light-induced phenomena in plasma conditions has increased. This is due to the fact that plasma, as a form of matter, prevails in the universe and, therefore, the light-induced phenomena are undoubtedly interesting to science. On the other hand, in laboratory plasma one can produce a sufficiently high concentration of excited atoms for the effective resonance interaction of these atoms with laser radiation. This sufficiently extends the number of chemical elements, which may be investigated with the help of modern lasers.

In a recent paper [7] we reported the observation of light-induced current (LIC) in the positive column of hydrogen glow discharge. In this case the LIC-signal was suppressed by a sufficiently stronger optogalvanic (OG) effect [8–10] and we detected the LIC-signal using the specific properties of LIC effect (the dependence of LIC on the frequency and direction of light propagation). As it was presented in [7], the voltage change in the positive column due to LIC was 1.5% of the one due to OG.

In the present work the theory of LIC in plasma is developed and the experimental results of investigation of LIC in rf discharge are presented. The influence of the OG effect may be significantly reduced or completely eliminated in this type of discharge and LIC may be measured in a more direct manner. Here, the results of investigating LIC in hydrogen and helium plasma of rf discharge are presented. We used laser radiation with frequencies corresponding to transition $n=2$ to $n=3$ (H_α absorption line with $\lambda=656.4$ nm) in hydrogen and to transition 2^1P-3^1D ($\lambda=667.8$ nm) in helium.

II. THEORY

The essence of the LIC effect can be explained by means of Fig. 1. Let us consider plasma which consists of electrons, ions, and neutral atoms. This plasma is illuminated with laser radiation having a wavelength corresponding to an atomic transition $n-m$ (level n, in particular, can be the atomic ground level). In the case of large Doppler broadening and narrow spectral width of laser radiation, the last induces the transition $n-m$ of those atoms only, whose velocity projections v_z on the wave vector **k** satisfy the following condition: $kv_z=\omega_L-\omega_{mn}\equiv\Omega$ (ω_L is the laser radiation frequency; ω_{mn} is the frequency of the atomic transition $n-m$). For this reason, the nonequilibrium additions occur in the velocity distributions $f_n(v_z)$ and $f_m(v_z)$ of atoms on the levels n and m (they are well known as Bennet gap and peak). Note that

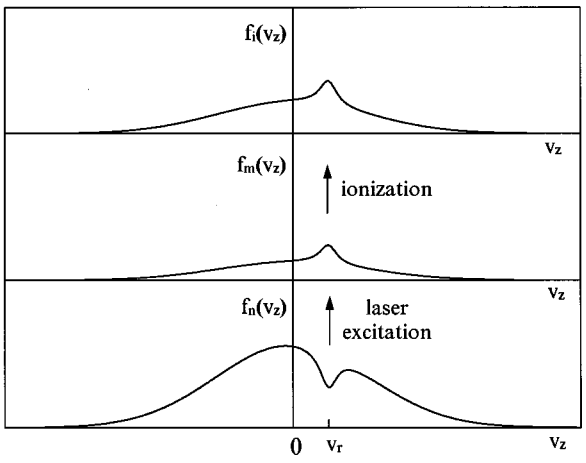

FIG. 1. Diagram illustrating the origin of light-induced current in plasma.

if $\omega_L \neq \omega_0$ these nonequilibrium additions are asymmetric with respect to $v_z=0$ and that means, particularly, that the excess of atoms in the state m has directed motion collinear to $\mathbf{k}$. Obviously, the velocity of this motion is $v_r=(\omega_L-\omega_{mn})/k=\Omega/k$. Since the atom in the state m is quite near to the ionization state, it is sufficiently easier to ionize an atom from this level than from the level n. Thus, we can assert here that all additional ions in plasma, which arise under the action of laser radiation, are mainly from the level m.

After ionization by collision with a light particle (an electron or photon) the ion has the same velocity as the atom before its ionization. This means that all the additional ions generated due to laser radiation have a directed motion collinear to $\mathbf{k}$ with velocity v_r. This is shown in Fig. 1 as the transfer of the Bennet peak from the atom velocity distribution $f_m(v_z)$ to the ion velocity distribution $f_i(v_z)$. The ions maintain a directed motion during the time τ_i until the first scattering or recombination. Electrons, which are also generated simultaneously with ions, lose their directed motion significantly faster than ions and make a negligible contribution to a charge transfer.

Thus LIC is the result of the transformation of the excited particles flux into a flux of ions. This transformation may occur due to the following reactions:

(i) Photoionization,

$$A^*+\hbar\omega=A^++e;$$

(ii) Electron impact ionization,

$$A^*+e=A^++e+e;$$

(iii) Associative ionization,

$$A^*+B=AB^++e,$$

(iv) Resonance charge exchange,

$$A^*+A^+=A^++A^*;$$

(v) Elastic collision of excited atom and ion,

$$A^*+A^+=A^*+A^+.$$

Note that the last two reactions do not change the total number of ions. The mechanism (v) of the translational motion transfer from atom subsystem to ion subsystem is caused by excited atoms having a larger collisional frequency due to their larger polarazability.

Now we shall consider a more detailed description of LIC. First, let us consider the kinetic equation for ions velocity distribution $f_i(\mathbf{v})$ under the homogeneous condition:

$$\frac{\partial}{\partial t}f_i(\mathbf{v})+\frac{e}{M_i}\mathbf{E}\cdot\frac{\partial}{\partial \mathbf{v}}f_i(\mathbf{v})=q_i(\mathbf{v})+\sum_k \nu^k f_k(\mathbf{v})+S_{ii}(\mathbf{v}) + S_{ia}(\mathbf{v})+\sum_k S_{ik}(\mathbf{v})-\nu^{\mathrm{rec}}f_i(\mathbf{v}). \tag{1}$$

In this equation $q_i(\mathbf{v})$ is the velocity nonselective source of ions; the terms, which describe the ionization income (with the rate ν^k) of atoms from some states k with nonequilibrium velocity distribution, are written separately. $S_{ii}(\mathbf{v})$ is the ion-ions elastic collision integral. The integral of ion-atom collision is also divided into two parts: $S_{ia}(\mathbf{v})$ and $\Sigma_k S_{ik}(\mathbf{v})$. The first of them describes the ion collision with the gas of neutral atoms which have equilibrium velocity distribution. The second one describes the ion collision with atoms occupying the states k and having nonequilibrium velocity distributions (this nonequilibrium may be caused by radiation absorption). The last term in Eq. (1) describes the recombination of charged particles at the rate ν^{rec}. Here we assume the atom is ionized without changing its velocity. This is valid if the atom ionization is caused by a nonelastic collision with a light particle (electron, photon) and this is not correct if this process is caused by a collision with a heavy particle, as in the case of associative ionization for instance. Below we will consider separately this specific case. In Eq. (1) we take into account the influence of a possible electric field $\mathbf{E}$ on the ion motion. We do not consider the collision between ions and electrons in Eq. (1), because the latter are light particles and cannot significantly affect the momentum of the ion subsystem.

Let us multiply Eq. (1) by $\mathbf{v}$ and integrate it over velocity. In the steady state case we obtain the equation for the ion flux:

$$\nu^{\mathrm{rec}}\mathbf{j}_i=\frac{e}{M_i}\mathbf{E}N_i+\sum_k \nu^k\mathbf{j}_k+\int \mathbf{v}S_{ia}(\mathbf{v})d\mathbf{v}+\sum_k \int \mathbf{v}S_{ik}(\mathbf{v})d\mathbf{v},$$

$$N_i=\int f_i(\mathbf{v})d\mathbf{v},\quad \mathbf{j}_i=\int \mathbf{v}f_i(\mathbf{v})d\mathbf{v},\quad \mathbf{j}_k=\int \mathbf{v}f_k(\mathbf{v})d\mathbf{v}. \tag{2}$$

Here N_i is the ion concentration, $\mathbf{j}_i$ is the ion flux, $\mathbf{j}_k$ is the flux of atoms in the state k. Deducing Eq. (2), we take into account that $\int \mathbf{v}q_i(\mathbf{v})d\mathbf{v}=0$ and $\int \mathbf{v}S_{ii}(\mathbf{v})d\mathbf{v}=0$ because ion-ion collisions do not change the total momentum of the ion subsystem. The term $\int \mathbf{v}S_{ia}(\mathbf{v})d\mathbf{v}$ in Eq. (2) describes the friction force for the ion flux in the gas of neutral atoms, which for clarity is considered as a motionless gas [11]. It is obvious that this force is directed against the ion flux and its value is proportional to the value of the ion flux [12]. Hence the following equation is valid:

$$\int \mathbf{v}S_{ia}(\mathbf{v})d\mathbf{v}=-\nu_i^{\mathrm{tr}}\mathbf{j}_i, \tag{3}$$

where ν_i^{tr} is the ion transport frequency with respect to collisions with atoms. Consequently, the terms $\int \mathbf{v}S_{ik}(\mathbf{v})d\mathbf{v}$ describe the friction force between the ion flux and the flux of atoms in the state k. In this case the more general equation than Eq. (3) is valid:

$$\int \mathbf{v}S_{ik}(\mathbf{v})d\mathbf{v}=-\nu_{ik}^{\mathrm{tr}}\mathbf{j}_i+\nu_{ki}^{\mathrm{tr}}\mathbf{j}_k, \tag{4}$$

where ν_{ik}^{tr} is the ion transport frequency with respect to collision with atoms in the state k and ν_{ki}^{tr} is the transport frequency of an atom in the state k for collisions with ions. These frequencies are related by the equation

$$\frac{\nu_{ik}^{\mathrm{tr}}}{N_k}=\frac{\nu_{ki}^{\mathrm{tr}}}{N_i}. \tag{5}$$

The first term on the right-hand side of Eq. (4) has the same sense as in Eq. (3) whereas the second term describes the ion drawing by excited particles flux. Using (2), (3), and (4), we obtain:

$$\mathbf{j}_i=\frac{\frac{e}{M_i}\mathbf{E}N_i+\Sigma_k\ (\nu^k+\nu_{ki}^{\mathrm{tr}})\mathbf{j}_k}{\nu^{\mathrm{rec}}+\nu_i^{\mathrm{tr}}+\Sigma_k\ \nu_{ik}^{\mathrm{tr}}}=\frac{e\tau_i}{M_i}\mathbf{E}N_i+\tau_i\sum_k\ (\nu^k+\nu_{ki}^{\mathrm{tr}})\mathbf{j}_k,$$

$$\tau_i=\frac{1}{\nu^{\mathrm{rec}}+\nu_i^{\mathrm{tr}}+\Sigma_k\ \nu_{ik}^{\mathrm{tr}}}. \tag{6}$$

This equation has clear meaning: the ion flux arises in plasma due to ion drift in the electrical field and as a result of momentum transfer from atom subsystem to ion subsystem due to collisions or ionization acts. Ionized atoms preserve their directed motion during an effective mean free time τ_i until the first collision with a neutral atom or until recombination. Usually a physical parameter such as ion mobility is used for the description of the ion drift in electrical field:

$$\mu_i=\frac{e\tau_i}{M_i}. \tag{7}$$

Let us compare the values of the ionization frequency ν^k and the transport frequency ν_{ki}^{tr} from Eq. (6) for the case of electron impact ionization. One has

$$\nu^k\sim N_e v_e\sigma_e^i,\quad \nu_{ki}^{\mathrm{tr}}\sim N_i v_i\sigma_{ki}, \tag{8}$$

where N_e is the electron concentration, v_e is the thermal electron velocity, σ_e^i is the cross section of atom ionization by electron impact, v_i is the thermal ion velocity, and σ_{ki} is the transport cross section of ion interaction with an atom in the state k. We restrict our consideration to quasineutral plasma where $N_e=N_i$. So, from Eq. (8) one can obtain

$$\frac{\nu_{ki}^{\mathrm{tr}}}{\nu^k}\sim\frac{v_i}{v_e}\frac{\sigma_{ki}}{\sigma_e^i}=\sqrt{\frac{T_i m}{T_e M_i}}\frac{\sigma_{ki}}{\sigma_e^i}\approx\sqrt{\frac{T_i}{T_e}}. \tag{9}$$

Here we take for estimations $\sqrt{m/M}\approx 10^{-2}$, $\sigma_e^i\approx 10^{-16}$ cm^2, $\sigma_{ki}\approx 10^{-14}$ cm^2.

Thus, according to Eq. (9) the electron impact ionization and the ion drawing effect may make comparable contributions to the ion flux in equilibrium plasma ($T_i=T_e$), but in gas discharge, where the electron temperature is much higher than the ion temperature, $\sqrt{T_i/T_e}\approx 10^{-1}$, the role of the ion drawing effect is negligible.

Note that electrons, which are generated simultaneously with ions, have on the average the same directed velocity and for the electron flux one can obtain an equation like (6),

$$\mathbf{j}_e=\frac{-\frac{e}{m}\mathbf{E}N_e+\Sigma_k\ (\nu^k+\nu_{ke}^{\mathrm{tr}})\mathbf{j}_k}{\nu^{\mathrm{rec}}+\nu_e^{\mathrm{tr}}+\Sigma_k\ \nu_{ek}^{\mathrm{tr}}}$$

$$=-\frac{e\tau_e}{m}\mathbf{E}N_e+\tau_e\sum_k\ (\nu^k+\nu_{ke}^{\mathrm{tr}})\mathbf{j}_k,$$

$$\tau_e=\frac{1}{\nu^{\mathrm{rec}}+\nu_e^{\mathrm{tr}}+\Sigma_k\ \nu_{ek}^{\mathrm{tr}}}, \tag{10}$$

where ν_e^{tr} is the electron transport frequency in plasma, ν_{ek}^{tr} is the transport frequency of electron collision with atoms in the state k, ν_{ke}^{tr} in opposite, is the transport frequency of atom in the state k with respect to collision with electrons, and τ_e is the effective mean free time of electron. In the case of ionization by electron impact, one can easily obtain by estimations similar to those from (9) that $\nu^k\sim\nu_{ke}^{\mathrm{tr}}$ and therefore both the ionization and electron drawing effect may give comparable contributions to electron flux.

The electrical current in plasma is determined by the difference between the ion and electron fluxes:

$$\mathbf{j}=\mathbf{j}_i-\mathbf{j}_e=(\mu_i+\mu_e)\mathbf{E}N_i+\sum_k\ (\tau_i-\tau_e)\nu^k\mathbf{j}_k$$

$$+\sum_k\ (\tau_i\nu_{ki}^{\mathrm{tr}}-\tau_e\nu_{ke}^{\mathrm{tr}})\mathbf{j}_k,$$

$$\mu_e=\frac{e\tau_e}{m}. \tag{11}$$

The first term on the right-hand side of Eq. (11) describes the well-known Ohm's law, whereas the second and third terms appear due to velocity nonequilibrium in the atom subsystem. Only these terms are of interest for us; hereafter for simplicity we will omit the term describing the charged particle drift in an electrical field.

However, one can always neglect the electron flux contribution to the light-induced current. Indeed, electrons have significantly larger transport collision frequency owing to a large difference between ion and electron masses.

$$\frac{\nu_e^{\mathrm{tr}}}{\nu_i^{\mathrm{tr}}}=\frac{v_e\sigma_{ea}}{v_i\sigma_{ia}}\approx\sqrt{\frac{M_i}{m}}\gg 1. \tag{12}$$

Here, it has been taken into account that for the polarazation potential of interaction of a charged particle and a neutral atom, the following relation between transport cross sections of an electron and an ion in collision with a buffer gas is valid:

$$\frac{\sigma_{ea}}{\sigma_{ia}}\approx\sqrt{\frac{T_i}{T_e}}. \tag{13}$$

According to (12), $\tau_i\gg\tau_e$; and LIC in plasma can be very accurately determined by the light-induced ion flux only:

$$\mathbf{j}^{\mathrm{LIC}}\approx\mathbf{j}_i. \tag{14}$$

Let us consider now the process of associative ionization as the result of the collision of an excited atom A^* and a buffer gas atom B which is accompanied by molecular ion AB^+ and electron generation.

$$A^*+B=AB^++e. \tag{15}$$

Kinetic equation for the molecular ions AB^+ can be written as (in the absence of applied electrical field **E**):

$$\frac{\partial}{\partial t}f_i(\mathbf{v})=q_i(\mathbf{v})+\sum_k \int w_k f_k(\mathbf{v}_1)f_B(\mathbf{v}_2) \times\delta\left(\mathbf{v}-\frac{M_A\mathbf{v}_1+M_B\mathbf{v}_2}{M_A+M_B}\right)d\mathbf{v}_1 d\mathbf{v}_2+S_{ia}(\mathbf{v}) +\sum_k S_{ik}(\mathbf{v})-\nu^{\mathrm{rec}}f_i(\mathbf{v}). \tag{16}$$

Here w_k is the probability of associative ionization for the atom A in the state k having collided with the particle B. For simplicity we assume w_k independence of the velocities of the scattered particles. The δ function in the integrand corresponds to momentum conservation (we neglect electron momentum), M_A and M_B are the masses of the particles A and B. Associative ionization usually plays an appreciable role in low temperature plasma where charged particles concentration is much less than that of neutral atoms. Therefore, in Eq. (16) we consider ion-atom collisions only. By multiplying on **v** and integrating over velocities in Eq. (16), one can get the following expression for the flux of molecular ions:

$$\mathbf{j}_i=\frac{M_A}{M_A+M_B}\tau_i\sum_k (\nu^k+\nu^{\mathrm{tr}}_{ki})\mathbf{j}_k, \quad \nu^k=N_B w^k, \tag{17}$$

where N_B is the concentration of buffer particles B. As can be seen from comparison of Eqs. (6) and (17) they diverge by the additional factor $M_A/(M_A+M_B)$ in Eq. (17). The origin of this factor in the case of associative ionization is rather clear.

The general formula for the light-induced ion flux, which fits the both cases, can be written as

$$\mathbf{j}_i^{\mathrm{LIC}}=\alpha\tau_i\sum_k (\nu^k+\nu^{\mathrm{tr}}_{ki})\mathbf{j}_k, \tag{18}$$

$\alpha=1$ for ionization by light particle,

$\alpha=M_A/(M_A+M_B)$ for associative ionization.

As could be seen from a quality picture of LIC origin (see Fig. 1), fluxes of atoms in states k (usually, two atomic states n and m adjasted by laser radiation) are created due to velocity-selective absorption of radiation and their values are not too different from one another (the important exception to this rule will be considered below). However, these atom fluxes give significantly unequal contributions to LIC because of a large difference between rates of atom ionization from these states. This difference of rates is due to their strong dependence on the energy of these states.

For instance, in the Thomson approximation [13] the cross-section of ionization by electron impact is proportional to I^{-2}, where I is the ionization energy for a given atomic level. Furthermore, due to the Boltzmann factor $\exp(-I/T_e)$ a larger number of electrons are capable of ionizing atoms from the upper level. Accordingly, for two atomic states with an energy difference in a few eV it is typical that the ionization rate from the upper atomic level is one order or more greater than the ionization rate from the lower level.

For associative ionization one often encounters situations when atom ionization is possible only from the upper level of interest and it is impossible from the lower level. In particular, in the present work we investigate LIC in helium and hydrogen where associative reactions can play the main role,

$$\mathrm{He}(3^1D)+\mathrm{He}=\mathrm{He_2}^++e, \tag{19}$$

$$\mathrm{H}(3)+\mathrm{H}=\mathrm{H_2}^++e, \tag{20}$$

however similar reactions with $\mathrm{He}(2^1P)$ and H(2) are energetically forbidden.

As a summation of this discussion, we can conclude that in many cases it is correct to neglect in Eq. (18) the terms corresponding to atom ionization from the lower (n) level of interest and to the ion drawing effect in nonequilibrium plasma.

Thus, the simple equation for the ion flux is valid:

$$\mathbf{j}^{\mathrm{LIC}}=\alpha\tau_i\nu^m\mathbf{j}_m. \tag{21}$$

To determine the flux of atoms A in the state m we have to consider several situations.

A. Isolated transitions $n-m$ (Fig. 1)

Here, we mean that radiation excites an atom from the state n to m from which the atom spontaneously decays back to the state n. An example of such a transition is the transition 2^1P-3^1D in He, which is experimentally investigated in this work (the helium transition 2^3P-3^3D also has the same property and was used for the OG effect studied in [10]).

The kinetic equation for the velocity distribution of atoms in the state m can be written as

$$\frac{\partial}{\partial t}f_m(\mathbf{v})+(\gamma_m+A_{mn})f_m(\mathbf{v})=q_m(\mathbf{v})+S_m(\mathbf{v})+p_{mn}(\mathbf{v}). \tag{22}$$

Here A_{mn} is the first Einstein coefficient for atom decay from the level m to the level n, γ_m is the frequency of an atom leaving the state m due to nonelastic collisions, in particular, ionization. The parameters $q_m(\mathbf{v})$ and $S_m(\mathbf{v})$ have the same meaning as in Eq. (1) for ions. The parameter $p_{mn}(\mathbf{v})$ is the probability for an atom with velocity **v** to absorb photon per unit time and volume (with an atom transit from the level n to m) [4]:

$$p_{mn}(\mathbf{v})=\frac{B_{nm}}{\pi}\int I(\Omega,\mathbf{n})\left(f_n(\mathbf{v})-\frac{g_n}{g_m}f_m(\mathbf{v})\right)\times\frac{\Gamma_{mn}}{\Gamma_{mn}^2+(\Omega-\mathbf{vn}\omega_{mn}/c)^2}d\mathbf{n}d\Omega. \quad (23)$$

In Eq. (23) $I(\Omega,\mathbf{n})$ is the spectral intensity of radiation spreading in the direction $\mathbf{n}$, Γ_{mn} is the homogeneous linewidth (half-width at half maximum, including natural and pressure broadening) corresponding to atom transition $n-m$, ω_{mn} is the frequency for this transition, $g_{n,m}$ are the statistical weights of the states n and m; B_{nm} is the second Einstein coefficient related with the first one by the equation

$$A_{mn}=\frac{\hbar\omega_{mn}^3 g_n}{2\pi^2c^2g_m}B_{nm}. \quad (24)$$

In our consideration we neglect the atom velocity change due to photon recoil.

In equilibrium and in the absence of radiation the particles in the upper and lower states have the Maxwellian velocity distribution $W_M(\mathbf{v})$,

$$f_{m,n}^0(\mathbf{v})=N_{m,n}^0W_M(\mathbf{v})=N_{m,n}^0\frac{1}{v_T^3\pi^{3/2}}\exp\left(-\frac{v^2}{v_T^2}\right),$$

$$v_T=\sqrt{\frac{2T}{M}}, \quad (25)$$

where $N_{m,n}^0$ are the concentrations of atoms in the states m or n, T is the gas temperature, M is the particle mass, v_T is their thermal velocity. As mentioned above, radiation creates nonequilibrium additions in the velocity distributions of atoms in the upper and lower states and therefore the macroscopic fluxes of atoms in these states. To calculate the value of the flux $\mathbf{j}_m$, let us multiply Eq. (22) by $\mathbf{v}$ and integrate it over velocities. Under steady state conditions we get the equation

$$(A_{mn}+\gamma_m)\mathbf{j}_m=\int\mathbf{v}S_m(\mathbf{v})d\mathbf{v}+\int\mathbf{v}p_{mn}(\mathbf{v})d\mathbf{v}. \quad (26)$$

For the friction force $\int\mathbf{v}S_m(\mathbf{v})d\mathbf{v}$ the relation similar to Eq. (3) holds. So, by means of this equation, we get

$$\mathbf{j}_m=\frac{\int\mathbf{v}p_{mn}(\mathbf{v})d\mathbf{v}}{A_{mn}+\gamma_m+\nu_m^{\mathrm{tr}}}, \quad (27)$$

where ν_m^{tr} is the transport frequency for particles in the state m. Calculation of $\int\mathbf{v}p_{mn}(\mathbf{v})d\mathbf{v}$ may be performed with the help of Eq. (23) where in linear approximation with respect to radiation intensity the equilibrium distributions (25) may be used. It is easy to obtain

$$\int\mathbf{v}p_{mn}(\mathbf{v})d\mathbf{v}=-\frac{v_T^2}{2}\frac{\omega_{mn}}{c}B_{nm}\left(N_n^0-\frac{g_m}{g_n}N_m^0\right)\times\int\mathbf{n}I(\Omega,\mathbf{n})\frac{d}{d\Omega}\Phi(\Omega)d\mathbf{n}d\Omega,$$

$$\Phi(\Omega)=\frac{1}{\pi}\int\frac{W_M(\mathbf{v})\Gamma_{mn}}{\Gamma_{mn}^2+(\Omega-\mathbf{vn}\omega_{mn}/c)^2}d\mathbf{v},\quad\int\Phi(\Omega)d\Omega=1. \quad (28)$$

Here $\Phi(\Omega)$ is the Voigt function which describes the shape of the broadened absorption line corresponding to the transition $n-m$. With the help of Eqs. (27) and (28) we get the following expression for the light-induced ion flux in plasma:

$$\mathbf{j}_i=-\alpha\frac{v_T^2}{2}\frac{\omega_{mn}}{c}\tau_i\frac{\nu^m}{A_{mn}+\gamma_m+\nu_m^{\mathrm{tr}}}B_{nm}\left(N_n^0-\frac{g_n}{g_m}N_m^0\right)\times\int\mathbf{n}I(\Omega,\mathbf{n})\frac{d}{d\Omega}\Phi(\Omega)d\mathbf{n}d\Omega. \quad (29)$$

Now we consider some approximations simplifying the formula (29). If the laser with spectral width of radiation much less than the broadened linewidth is used as the radiation source, the spectral intensity may be considered to be a monochromatic one,

$$I(\Omega,\mathbf{n})=I_L\delta(\Omega-\Omega_L)\delta(\mathbf{n}-\mathbf{n}_L), \quad (30)$$

where I_L is the laser radiation intensity and $\Omega_L,\mathbf{n}_L$ are the radiation frequency detuning from the center of the absorption line and the radiation spreading direction, respectively. With the help of Eq. (30) the integration in Eq. (29) over the frequency and direction of radiation spreading can be easily performed:

$$\mathbf{j}_i=-\mathbf{n}_L\alpha\frac{v_T^2}{2}\frac{\omega_{mn}}{c}\tau_i\frac{\nu^m}{A_{mn}+\gamma_m+\nu_m^{\mathrm{tr}}}B_{nm}\times\left(N_n^0-\frac{g_n}{g_m}N_m^0\right)I_L\frac{d}{d\Omega_L}\Phi(\Omega_L). \quad (31)$$

Note here the important moment, specific for LIC. As a function of the detuning (Ω_L) the ion flux $\mathbf{j}_i$ is the derivative of the Voigt contour $\Phi(\Omega_L)$ with respect to Ω_L. As can be seen from Eq. (31), the flux $\mathbf{j}_i$ is an antisymmetric function of Ω_L.

Further, it is typical for the spontaneous rates of atom decay to be significantly larger than the collision rates $(A_{mn}\gg\gamma_m+\nu_m^{\mathrm{tr}})$. This fact, along with Eq. (24), allows us to write (31) as

$$\mathbf{j}_i=-\mathbf{n}_L\alpha\frac{\pi^2v_T^2c}{\hbar\omega_{mn}^2}\tau_i\nu^m\frac{g_m}{g_n}\left(N_n^0-\frac{g_n}{g_m}N_m^0\right)I_L\frac{d}{d\Omega}\Phi(\Omega_L). \quad (32)$$

In this approximation the magnitude of the ion flux and therefore of LIC does not depend upon line strength. That means, for instance, that for two isolated atom transitions, which greatly differ one from another by their strength, LIC's which are equal in magnitude may be induced.

In the case of large Doppler broadening the following approximation for the Voigt function can be used:

$$\Phi(\Omega)\approx\frac{1}{\sqrt{\pi}\omega_D}\exp\left[-\left(\frac{\Omega}{\omega_D}\right)^2\right],$$

$$\frac{d}{d\Omega}\Phi(\Omega)\approx-\frac{2\Omega}{\sqrt{\pi}\omega_D^3}\exp\left[-\left(\frac{\Omega}{\omega_D}\right)^2\right]=-\frac{2\Omega}{\omega_D^2}\Phi(\Omega), \tag{33}$$

$$\omega_D=\frac{v_T}{c}\omega_{mn}.$$

The maximal value of $|d\Phi(\Omega)/d\Omega|=\sqrt{2}/(\sqrt{\pi}\omega_D^2)\exp(-1/2)$ is achieved at $\Omega=\pm\omega_D/\sqrt{2}$, where ω_D is the Doppler width of the absorption line. Consequently, the maximal value of LIC is

$$\mathbf{j}_i^{\max}=-\mathbf{n}_L\alpha\frac{\pi^2c^3}{\hbar\omega_{mn}^4}\sqrt{\frac{2}{\pi}}e^{-1/2}\tau_i\nu^m\frac{g_n}{g_m}\left(N_n^0-\frac{g_m}{g_n}N_m^0\right)I_L. \tag{34}$$

Note that in these approximations, according to Eq. (34) the magnitude of LIC does not depend on the thermal velocity of atoms.

To compare the theoretical and experimental data it is convenient to connect the LIC value with the absorption power of laser radiation $W(\Omega)$ per volume unit:

$$W(\Omega)=\hbar\omega_{mn}\int p_{mn}(\mathbf{v})d\mathbf{v}$$

$$=\hbar\omega_{mn}B_{nm}I_L\left(N_n^0-\frac{g_m}{g_n}N_m^0\right)\Phi(\Omega). \tag{35}$$

With the help of Eqs. (31) and (35) one can get

$$\mathbf{j}_i=-\mathbf{n}_L\alpha\tau_i\frac{v_T^2}{2\hbar c}\frac{\nu^m}{A_{mn}+\gamma_m+\nu_m^{\mathrm{tr}}}\frac{d}{d\Omega}W(\Omega). \tag{36}$$

In the case of large Doppler broadening and by using Eq. (33) this equation can be written as:

$$\mathbf{j}_i=\mathbf{n}_L\tau_i\alpha v_T\frac{\Omega}{\omega_D}\frac{\nu^m}{A_{mn}+\gamma_m+\nu_m^{\mathrm{tr}}}\frac{W(\Omega)}{\hbar\omega_{mn}}. \tag{37}$$

Equation (37) has a form which is the most convenient for the physical meaning of LIC being made clear. Indeed, the factor $\dot{N}_m=W(\Omega)/(\hbar\omega_{mn})$ is the number of atoms excited in the state m by light per time and volume units. The velocity of these excited atoms is $v_T\Omega/\omega_D$. Only the portion $\xi=\nu^m/(A_{mn}+\gamma_m+\nu_m^{\mathrm{tr}})$ of these excited atoms gets ionized, before leaving this state due to spontaneous decay, inelastic collisions or elastic ones with a change of atom velocity. Therefore, $\dot{N}_i=\xi\dot{N}_m$ is the additional source of ions generated with the directed velocity $v_i=\alpha v_T\Omega/\omega_D$. The ions maintain this motion during the time τ_i. The concentration of ions, which have directed motion, is $\tau_i\dot{N}_i$ and the ion flux is $j_i=v_i\tau_i\dot{N}_i$.

Equation (37) was deduced in linear approximation with respect to radiation intensity. However, it can be shown in a similar manner as in [14] that this formula is valid at an arbitrary radiation intensity and under weak restriction on relaxation details. In other words, the LIC magnitude is proportional to absorbed power of radiation. In particular, for comparing experimental data it is convenient to use the ratio of the LIC amplitude to the density of the absorbed radiation power at the line center,

$$\eta=\frac{i_{\mathrm{LIC}}^{\max}}{P(0)}=\frac{ej_i^{\max}}{W(0)}=\frac{e^{-1/2}}{\sqrt{2}}\alpha\tau_i\frac{ev_T}{\hbar\omega_{mn}}\frac{\nu^m}{A_{mn}+\gamma_m+\nu_m^{\mathrm{tr}}},$$

$$i_{\mathrm{LIC}}=ej_is_L. \tag{38}$$

Here s_L is the cross-section of a laser beam and $P(0)=W(0)s_L$ is the absorbed light power in plasma per length unit. The value η describes the effectiveness of the light power transformation into the electrical current.

B. Case of collisional mixing of several atomic states

Now we consider the system of atomic states, which consists of two groups of the nearest levels of the upper m and lower n states. There are optical transitions between the separate states of upper and lower groups. We assume that energy differences between the states inside both groups are small ($<T$), thus there is an effective mixing inside these groups due to the collision of atoms. This situation takes place, for instance, for the hydrogen transition which corresponds to the H_α line. It is well known [15] that this line is formed by seven spectral components.

To calculate the flux of atoms in the upper group of states, we use the kinetic equation:

$$\frac{\partial}{\partial t}f_m(\mathbf{v})+\left(\gamma_m+\sum_n A_{mn}\right)f_m(\mathbf{v})$$

$$=q_m(\mathbf{v})+S_m(\mathbf{v})+\sum_n p_{mn}(\mathbf{v})$$

$$+\sum_{m'}[\nu_{m'm}f_{m'}(\mathbf{v})-\nu_{mm'}f_m(\mathbf{v})]. \tag{39}$$

Here $\nu_{mm'}$ is the collision frequencies of atom transition from a state m to a state m'. For simplicity we assume that atom velocity does not change under these collisions and $\nu_{mm'}=\nu_{m'm}=\nu_m$. Other parameters have meanings similar to those from Eq. (22). By multiplying Eq. (39) on $\mathbf{v}$ and integrating it over velocities, one can obtain

$$(A_m+\gamma_m+\nu_m^{\mathrm{tr}}+\nu^{(m)})\mathbf{j}_m=\int\mathbf{v}p_m(\mathbf{v})d\mathbf{v}+\nu_m\mathbf{j}_{\mathrm{up}}. \tag{40}$$

Here we introduce the notations

$$A_m=\sum_n A_{mn},\quad p_m(\mathbf{v})=\sum_n p_{mn}(\mathbf{v}),$$

$$\nu^{(m)}=\sum_{m'}\nu_{mm'},\quad \mathbf{j}_{\mathrm{up}}=\sum_m\mathbf{j}_m. \tag{41}$$

Using Eq. (40), we find the total flux of atoms in the upper group of states,

$$\mathbf{j}_{\rm up}=\left(1-\nu_m\sum_m \frac{1}{A_m+\gamma_m+\nu_m^{\rm tr}+\nu^{(m)}}\right)^{-1} \times\sum_m \frac{\int \mathbf{v}p_m(\mathbf{v})d\mathbf{v}}{A_m+\gamma_m+\nu_m^{\rm tr}+\nu^{(m)}}. \quad (42)$$

If the collision mixing inside of the upper group of atom states is efficient ($\nu^{(m)}\gg A_m+\gamma_m+\nu_m^{\rm tr}$), Eq. (42) may be simplified:

$$\mathbf{j}_{\rm up}=\frac{\Sigma_m\int \mathbf{v}p_m(\mathbf{v})d\mathbf{v}}{\frac{1}{m}\sum_m (A_m+\gamma_m+\nu_m^{\rm tr})}. \quad (43)$$

Here m is the number of states in the upper group. Further, in a similar manner as in the previously derived Eq. (36) one can get the expression for LIC,

$$\mathbf{j}_i=-\mathbf{n}_L\alpha\tau_i\frac{v_T^2}{2\hbar c}\frac{\nu^m}{\langle A_m+\gamma_m+\nu_m^{\rm tr}\rangle}\frac{d}{d\omega}W(\omega),$$

$$\langle A_m+\gamma_m+\nu_m^{\rm tr}\rangle=\frac{1}{m}\sum_m (A_m+\gamma_m+\nu_m^{\rm tr}),$$

$$W(\omega)=\hbar\omega\sum_{m,n}\int p_{mn}(\mathbf{v})d\mathbf{v}. \quad (44)$$

Here $W(\omega)$ is the total absorbed radiation power over all transitions.

Thus, if the atomic levels are strongly mixed, then all states of the upper group are combined into one effective state with a mean relaxation rate. If the absorption line has a complex structure due to contributions of several atom transitions, then, according to Eq. (44), the dependence of LIC on the light frequency is complex too. This case, in particular, is near the absorption line H_α in hydrogen. However, as in the case of the isolated atomic transition, LIC dependence on frequency is given by the frequency derivative of the absorption line shape. This is very convenient for experimental LIC identification.

C. Λ-type transition in a three level atom system

This type of atomic transition is important in discharging gases which have metastable states quite near ionization states. The concentration of atoms in these states may be sufficiently high to affect the discharge. The laser radiation excites atoms from a metastable state to an upper state, from which the atoms rapidly decay directly or nondirectly to the ground state. Due to this mechanism the concentration of metastable atoms may be significantly decreased in discharge. This is the reason for the well-known ''negative'' OG effect, which was observed, for instance, in Ne [16]. If the laser radiation acts on atoms in a velocity-selective way, then the Bennet gap is created in velocity distribution of metastable atoms and, therefore, the flux of metastable atoms is induced. Because metastable atoms are ionizied easier than atoms in the ground states, the flux of metastable atoms induces an ion flux.

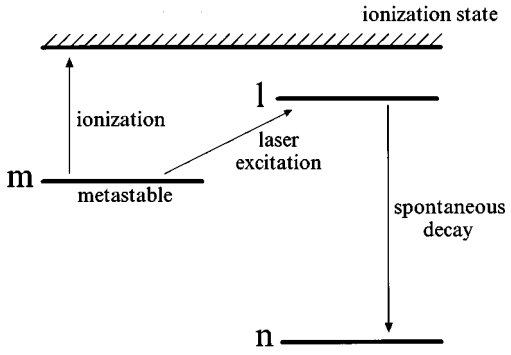

FIG. 2. Schematic energy diagram illustrating the origin of LIC in the case of a three-level atom system.

Let us consider the kinetic equations which describe the three level system (see Fig. 2). For our goals it is enough to write equations only for atoms in m and l states, because one can neglect the contribution of the ground atom flux to ion current:

$$\frac{\partial}{\partial t}f_m(\mathbf{v})+\gamma_m f_m(\mathbf{v})=q_m(\mathbf{v})+S_m(\mathbf{v})-p_{lm}(\mathbf{v})+A_{lm}f_l(\mathbf{v}), \quad (45)$$

$$\frac{\partial}{\partial t}f_l(\mathbf{v})+(A_{lm}+A_{\rm ln}+\gamma_l)f_l(\mathbf{v})=q_l(\mathbf{v})+S_l(\mathbf{v})+p_{lm}(\mathbf{v}). \quad (46)$$

Under steady state conditions we can obtain the equations for atom fluxes in m and l states:

$$(\gamma_m+\nu_m^{\rm tr})\mathbf{j}_m=-\int \mathbf{v}p_{lm}(\mathbf{v})d\mathbf{v}+A_{lm}\mathbf{j}_l, \quad (47)$$

$$(A_{lm}+A_{\rm ln}+\gamma_l+\nu_l^{\rm tr})\mathbf{j}_l=\int \mathbf{v}p_{lm}(\mathbf{v})d\mathbf{v}. \quad (48)$$

Finally, from these equations we obtain the values of the fluxes:

$$\mathbf{j}_m=-\frac{A_{\rm ln}+\gamma_l+\nu_l^{\rm tr}}{A_{lm}+A_{\rm ln}+\gamma_l+\nu_l^{\rm tr}}\frac{\int \mathbf{v}p_{lm}(\mathbf{v})d\mathbf{v}}{\gamma_m+\nu_m^{\rm tr}}, \quad (49)$$

$$\mathbf{j}_l=\frac{\int \mathbf{v}p_{lm}(\mathbf{v})d\mathbf{v}}{A_{lm}+A_{\rm ln}+\gamma_l+\nu_l^{\rm tr}}. \quad (50)$$

As can be seen from Eqs. (49) and (50), the flux $\mathbf{j}_m$ of metastable atoms is $(A_{\rm ln}+\gamma_l+\nu_l^{\rm tr})/(\gamma_m+\nu_m^{\rm tr})$ times greater than the flux $\mathbf{j}_l$ of atoms in l state (if $A_{\rm ln}\gg\gamma_m+\nu_m^{\rm tr}$). Therefore, despite the fact that atoms in the state l are closer to the ionized state, the main contribution in LIC is given by the flux of metastable atoms. With the help of the expression for $\int \mathbf{v}p_{lm}(\mathbf{v})d\mathbf{v}$ (28), we get the value of LIC in this case:

$$\mathbf{j}_i=\mathbf{n}_L\alpha\tau_i\frac{v_T^2}{2\hbar c}\frac{\nu^m}{\gamma_m+\nu_m^{\rm tr}}\frac{A_{\rm ln}+\gamma_l+\nu_l^{\rm tr}}{A_{lm}+A_{\rm ln}+\gamma_l+\nu_l^{\rm tr}}\frac{d}{d\Omega}W(\Omega). \quad (51)$$

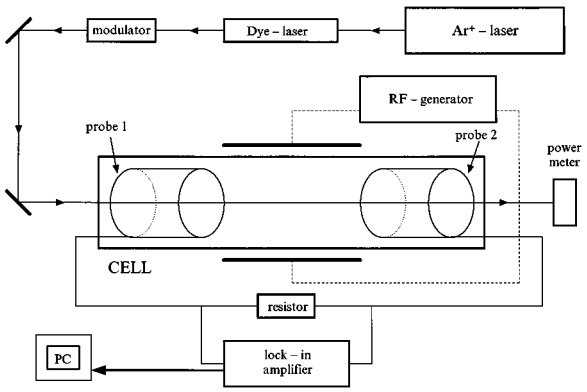

FIG. 3. Experimental configuration for measuring LIC in rf discharge.

It is a typical situation, when $A_{\ln} \gg A_{lm}, \gamma_l, \nu_l^{\mathrm{tr}}$. Therefore, the factor $(A_{\ln}+\gamma_l+\nu_l^{\mathrm{tr}})/(A_{lm}+A_{\ln}+\gamma_l+\nu_l^{\mathrm{tr}})$ in Eq. (51) may be substituted by 1. The comparison of this formula and Eq. (36) shows that LIC, which is due to ionization of metastable atoms, has the opposite sign to LIC in the case described by Eq. (36). Besides, the ionization efficiency $\nu^m/(\gamma_m+\nu_m^{\mathrm{tr}})$ in the case of metastable atoms may be significantly larger than $\nu^m/(A_{mn}+\gamma_m+\nu_m^{\mathrm{tr}})$ in the case described by Eq. (36). This means that for the same level of absorbed radiation power the magnitude of LIC under the described conditions may be significantly larger than the one in the case of isolated transition in two level system.

III. EXPERIMENT

A. Method of LIC measurement

In our previous work [7] LIC was induced in a positive column of hydrogen glow discharge with the help of laser radiation spreading collinear to the electrical field in the positive column. The LIC-signal was detected by a voltage change on a ballast resistor. However, together with the LIC-signal the OG-signal was detected, which was approximately two orders larger than the LIC-signal. In order to eliminate the influence of the OG effect we used in [7] the method of subtraction of the two signals corresponding to two alternating laser beams which counterpropagate in the cell.

In the present work we use rf discharge, which in its own nature should not create any constant electrical field. Therefore, the hope arises that it helps to exclude the manifestation of OG effect appreciably. Discharge was created with a field directed orthogonally to the light propagation. The probes were symmetrical with regard to the discharge plasma (Fig. 3).

The method of LIC detection was in the following. It is well known that on any probe in plasma the fluxes of ions and electrons fall. The isolated probe obtains some negative potential relative to plasma so that these fluxes are compensated in their magnitudes. This potential increases if the ion flux falling on the probe is increased by some method. Because LIC is an ion flux and if this flux falls fully on the probe, then the potential of this probe increases by the value

$$\Delta U^{\mathrm{probe}} = \frac{dU^{\mathrm{probe}}(i)}{di} i_{\mathrm{LIC}} = R^{\mathrm{probe}} i_{\mathrm{LIC}}, \tag{52}$$

where $U^{\mathrm{probe}}(i)$ is the current-voltage characteristic of the probe and $R^{\mathrm{probe}} = dU^{\mathrm{probe}}(i)/di$ is its dynamical resistance.

In the experiment we use two hole probes which are on both sides of the plasma gap and are in contact with plasma. The laser beam spreads through both probes, so LIC was directed from one probe to another. Therefore, the potential of the first probe increases and the potential of the other probe decreases relative to adjoined plasma. Besides, there is a voltage in the plasma column due to the ion current. As a result, the voltage between probes arises:

$$\Delta U = (R_1^{\mathrm{probe}} + R^{\mathrm{pl}} + R_2^{\mathrm{probe}}) i_{\mathrm{LIC}} = R_c i_{\mathrm{LIC}}, \tag{53}$$

where $R_{1,2}^{\mathrm{probe}}$ are the dynamic resistance of the probes, R^{pl} is the resistance of the plasma gap between these probes [10], and R_c is the whole cell resistance.

If these probes are connected by a circuit with the ballast resistor R^b, then in the circuit the current is generated:

$$i = \frac{R_c}{R_c + R^b} i_{\mathrm{LIC}}. \tag{54}$$

This current is convenient to detect by measuring the voltage on the given ballast resistor. According to (54), if one chooses $R^b \ll R_c$, then the detected current should be equal to i_{LIC} with a high accuracy. We try to attain this condition to avoid the permanent control of the value R_c in the experiment.

B. Experimental setup

The experimental setup used for investigation of LIC is shown in Fig. 3. In the glass cell with the inner radius $R = 0.2$ cm the high frequency ($f = 800$ MHz) discharge is induced in a transverse direction. Two hole probes are in contact with the plasma and are spaced 5 cm apart. The cell is coupled to a diffusion pump system which can provide a vacuum of about 10^{-6} torr. The cell is filled with spectral clean helium or hydrogen. The gas pressure in the cell can be changed beginning from parts of torr.

In the experiment we used a dye laser operating on DCM dye pumped by an argon laser. The dye laser was tuned over the absorption line of helium or hydrogen by an intracavity Fabry-Perot etalon. The typical laser power was 150 mW near the H_α line ($\lambda = 656.4$ nm) and 70 mW near $\lambda = 667.8$ nm (helium transition $2^1P - 3^1D$). Laser beam was modulated with 23 Hz frequency by an electro-optical modulator and entered into the discharge tube through the hole probes and a plasma column. In the exit of the tube the laser beam falls on a power meter. The probes were closed by an external circuit with the ballast resistor of 3300 Ω. The measurement of the ballast resistor voltage was performed with a selective voltmeter on the frequency of radiation intensity modulation. The data from the laser beam power meter and selective voltmeter were recorded by a computer.

The goal of the experiment was the measurement of the ballast resistor voltage and of the absorbed power of laser radiation in relation to the frequency detuning, intensity of laser radiation, and gas pressure.

C. Experimental results and discussion

The total resistance R_c of the discharge cell was measured by two methods. In the first method we measured current dependence on R^b with the laser on. Assuming that this dependence is described by Eq. (54), we calculate R_c. In the second method the current in the circuit was created by an external supply with the laser off. At a given applied voltage we measured the circuit current and calculated straightforward the resistance R_c. Both methods gave equal magnitudes of R_c. Depending on the gas sort and its pressure the magnitude of R_c was varied from 30 KΩ to 150 KΩ. We used the fixed ballast resistor $R^b = 3.3$ KΩ in all cases that could give error in the measurement of i_{LIC} not greater than 10% in the worst case. The application of ballast resistors of two different values allowed us to eliminate this error.

The experiments were performed in a wide range of gas pressure (from 0.1 torr to 6 torr) in the discharge cell and in an accessible interval of laser power. Several times we recorded the dependence of ballast resistor voltage and the absorbed laser power versus the laser frequency at fixed setup parameters. The signal of absorbed power was obtained as a result of the computer subtraction of the light powers at the cell's input and output. This operation was performed in real time scale and allowed us to decrease significantly the influence of laser instability under conditions when radiation absorption was weak. Besides the absorbed radiation power we measured the fluorescence intensity as a function of the laser frequency.

It revealed in experiment that there was some region of pressure near 1 torr for He and 0.3 torr for H where the profiles of current dependence on detuning were very close to the frequency derivative of absorption line shape and, hence, corresponded to the pure LIC manifestation. The sign of the signal also corresponds to the sign of i_{LIC}. The change of the direction of light propagation to its opposite led to the signal sign change. All these facts allow us to state that under this condition we observed the light-induced current effect and, moreover, without OG effect revealing. The typical current signals and absorption line shapes for He and H at ''optimal'' values of gas pressure are shown in Figs. 4(a) and 4(b). The curves corresponding to LIC are obtained as a result of direct signal recording. The absorption line shapes were obtained by computer processing of several measurements of absorbed light power and spontaneous emission intensity. The frequency scale was determined by the Fabry-Perot etalon. Because there is an isolated absorption line in helium, the LIC-signal has a very simple form: the curve is antisymmetric and has a sole intersection with the x axis. In the case of hydrogen, LIC-signal is more intricate and expressive in accordance with the compound (several spectral components) shape of the H_α line. This curve meets the x axis several times and, as it must be, the integral of LIC-signal over frequency is very close to zero.

Outside the region of ''optimal'' pressure we observed a current signal additional to that one predicted by LIC theory. The shape of this additional signal coincided with the shape of the absorption line, which is typical for OG effect. We should note here that under condition of rf discharge such a kind of signal was observed in an earlier work [22]. In that work the nature of this signal, called ''optovoltaic,'' was

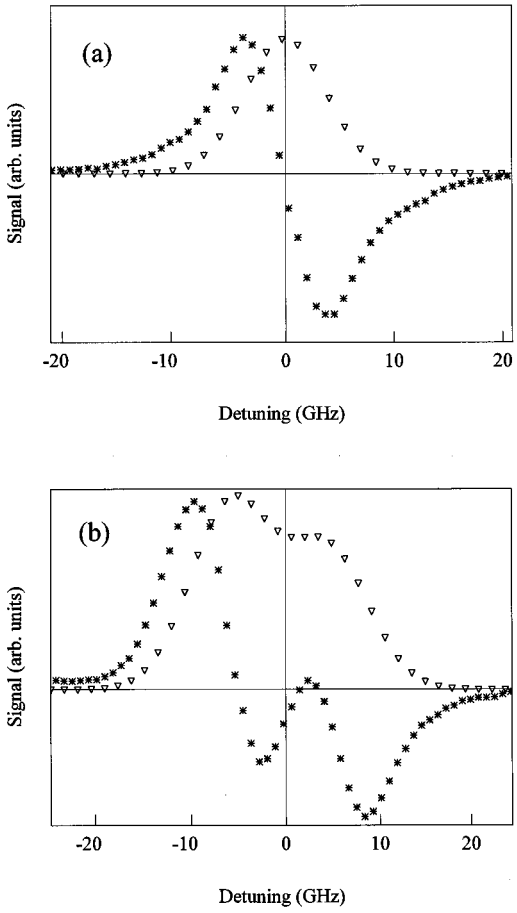

FIG. 4. Experimental data on LIC signal (*) and spontaneous emission intensity (∇) vs laser radiation detuning; (a) in helium, (b) in hydrogen.

connected with the depletion of metastable atom population via optical pumping and, therefore, a decrease of the electron ejection rate from one of the probes when it is struck by metastable atoms. In our experiment the laser radiation did not act on atoms of He or H at metastable levels but, on the contrary, a signal like the OG-signal was detected. It was not our goal to investigate the nature of this additional signal. We supposed that this is a variety of the OG effect and, moreover, the full symmetry of electrodes and discharge was not achieved in our experiments. This additional signal we excluded by computer processing of experimental data using the specific distinctive features of LIC- and OG-signals. Actually, OG-signal repeats the shape of the absorption line and, in particular, it does not change its sign with the change of the detuning sign. As was mentioned above, LIC-signal follows the absorption line frequency derivative profile and has, in principle, sign-changing behavior as a function of the laser frequency detuning. The integral of LIC-signal over detuning should equal zero. The processing consisted in subtracting some signal, which is proportional to absorption line, from the experimental signal. The magnitude of weight factor was chosen so that the integral of the residual signal over detuning was equal to zero. Tests show that the residual signal is close to the derivative profile of the absorption line. Thus, we can conclude this residual signal corresponds to LIC effect. Such processing allowed us to make the correct measurements of LIC-signal under conditions when the

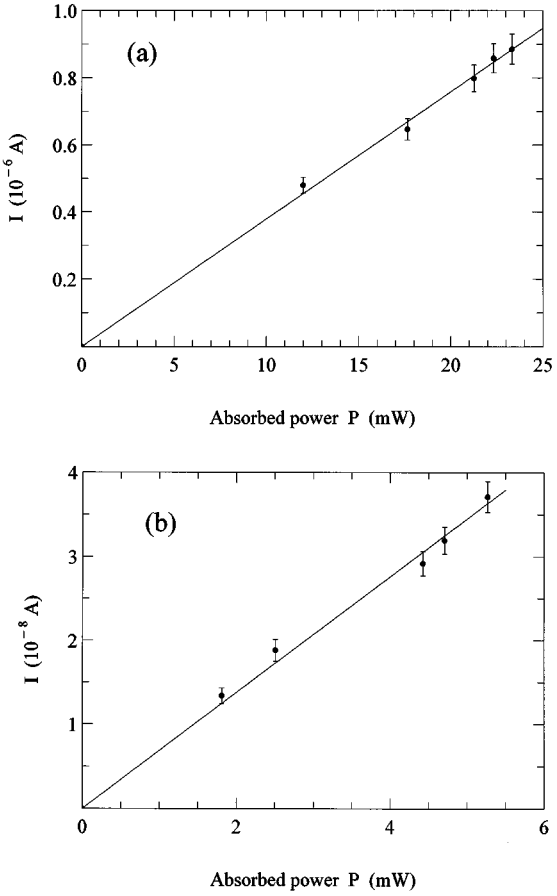

FIG. 5. Measured LIC as a function of absorbed radiation power; (a) in helium, (b) in hydrogen.

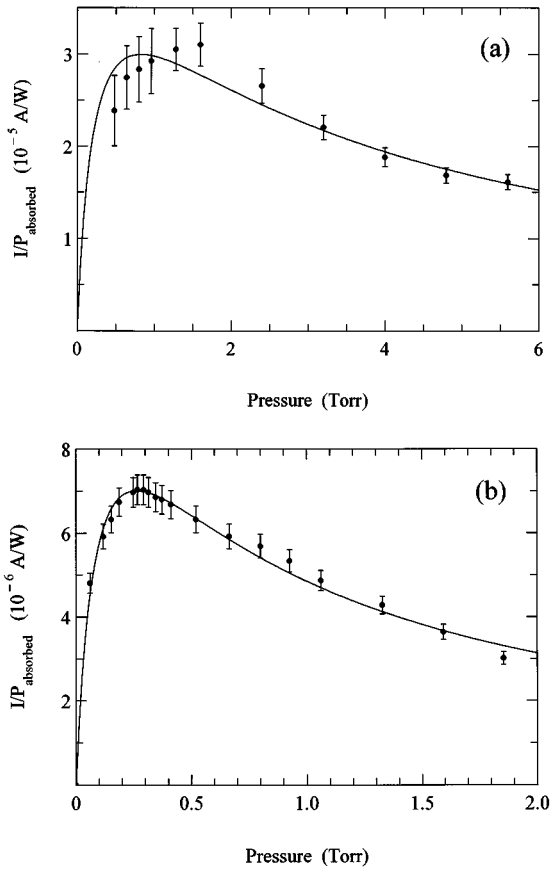

FIG. 6. LIC normalized on absorbed radiation power as a function of gas pressure. Fitted curve $\eta(p)$ is shown by a solid line; (a) in helium, (b) in hydrogen.

masked OG effect exists. The magnitude of the last one was different at different gas pressure, but was never significantly larger than the magnitude of LIC-signal.

Also it was noticed in experiments that any deviation of beam propagation from the center of the cell led to increasing of OG-signal magnitude, which was undesirable. Therefore we tried to direct the laser beam exactly along the cell's axis.

An increase of laser beam diameter by $1\frac{1}{2}$ did not lead to a noticeable change in magnitude of detected current under the same value of absorbed laser radiation power.

The theory developed in the preceding section predicted the proportionality of LIC magnitude to the absorbed radiation power [see Eq. (37)]. We have performed some measurements to test this statement. The results of these experiments are presented in Figs. 5(a) and 5(b). Here the magnitude of LIC (half difference in maximal and minimal values of LIC function on detuning) is shown versus the absorbed light power $P(0)$ at the line center. In both cases the experimental data lie on a straight line. So theory and experiment agree in this point as well. The maximal obtained values of i_{LIC} were the following: $i_{\mathrm{LIC}}^{\max}=4\times10^{-8}$ A at $p=0.265$ torr and at absorbed light power per length unit $P(0)=1$ mW/cm for hydrogen, and $i_{\mathrm{LIC}}^{\max}=10^{-6}$ A at $p=0.96$ torr and at absorbed light power per length unit $P(0)=4.6$ mW/cm for helium.

The dependencies of $\eta=i_{\mathrm{LIC}}/P(0)$ on gas pressure are shown in Fig. 6(a) (helium) and Fig. 6(b) (hydrogen). As can be seen from these pictures, in both cases the LIC-signal normalized on the absorbed power increases in the beginning with the pressure increase, acquires its maximum, and then decreases. Such a kind of normalized LIC-signal behavior has an adequate explanation if one assumes that ionization is due to an associative mechanism. Indeed, because the frequency of associative ionization and transport collision frequencies are proportional to gas pressure, Eq. (38) can be written as

$$\eta(p)=\frac{e^{-1/2}}{\sqrt{2}}\alpha\frac{ev_T}{\hbar\omega_{mn}}\frac{1}{\nu^{\mathrm{rec}}+p\overline{\nu_i^{\mathrm{tr}}}}\frac{p\overline{\nu^m}}{A_{mn}+\gamma_m^0+p\overline{\nu^{\mathrm{col}}}}, \tag{55}$$

where $\overline{\nu^m},\overline{\nu_i^{\mathrm{tr}}},\overline{\nu^{\mathrm{col}}}$ are the frequencies of corresponding processes at $p=1$ torr, and p is the gas pressure measured in torr units. In Eq. (55), ν^{rec} is the rate of charged particles recombination, and γ_m^0 is the part of γ_m, that does not depend on gas pressure and is caused by the possible spontaneous decay of the atom in the state m to other, different from n, states, photoionization or electron impact ionization. As will be shown below, the last two processes may be neglected under our experimental conditions. Therefore $\gamma_{3^1D}^0=0$ for helium and $\gamma_3^0=A_{31}=5.58\times10^7\ \mathrm{s}^{-1}$ for hydrogen. Furthermore, in our experiment recombination takes

place on the wall of the cell and, in general, $\nu^{\rm rec}$ also depends on gas pressure with its maximal value $\nu^{\rm rec}(0)$ at $p=0$ and decreasing with pressure increase. However, in Eq. (55) we neglect this dependence, assuming $\nu^{\rm rec}=\nu^{\rm rec}(0)$ for any pressure, because the error in $\nu^{\rm rec}$, arising with pressure increase, does not exert any strong influence on the error of the parameter $1/(\nu^{\rm rec}+p\overline{\nu_i^{\rm tr}})$ on the background of increasing $p\overline{\nu_i^{\rm tr}}$.

As can be seen from Eq. (55), with increasing pressure the value of $\eta(p)$ also initially increases, acquires its maximum, and then decreases tending to p^{-1} low at large values of pressure. Thus, the behaviors of $\eta(p)$ and the experimental data agree qualitatively.

The rates of other mechanisms of helium and hydrogen ionization from the state $n=3$ (by electron impact or photoionization) do not explicitly depend on pressure like (55) and, therefore, cannot explain the increasing part of $\eta(p)$. Moreover, these rates do not provide, as we will see below, the experimentally observed magnitude of LIC.

We tried to calculate the function $\eta(p)$ for helium plasma using known data on processes which have an influence on LIC.

It is a well-known fact that in discharge plasma in helium the main mechanism of the ionization of helium atom from the state 3^1D is the associative ionization caused by collision with helium atoms in the ground state [reaction (19)]. The cross-section of this process was measured in the work [17]: $\sigma^{\rm He(3^1D)}=2\times10^{-15}$ cm^2. The ionization rate corresponding to this cross-section at $T=300$ K, is

$$\overline{\nu^{\rm He(3^1D)}}=11.3\times10^6\ \ {\rm s}^{-1}\ {\rm torr}^{-1}. \tag{56}$$

Note, for comparison, that the rate of ionization by electron impact at $n_e=10^{11}$ cm^{-3}, $v_e=10^8$ cm/s and at a rather heightened value of the cross-section of this process $\sigma=10^{-15}$ cm^2 is $\nu=10^4$ s^{-1}. This value is three orders less than the one for associative ionization (56) at gas pressure 1 torr. The rate of photoionization at applied laser radiation intensity is $\nu=10^3$ s^{-1} and is even less than the electron impact ionization rate.

We find the transport frequency $\overline{\nu^{\rm tr}_{\rm He_2^+}}$ by using the known mobility of $\rm He_2^+$: $\mu_{\rm He_2^+}=1.15\times10^4/p$ cm^2 V^{-1} s^{-1} [18] and Eq. (7):

$$\overline{\nu^{\rm tr}_{\rm He_2^+}}=8\times10^6\ \ {\rm s}^{-1}\,{\rm torr}^{-1}. \tag{57}$$

The equation for recombination rate is valid:

$$\nu^{\rm rec}=\beta\nu^{\rm rec}_{\rm TL},\quad \nu^{\rm rec}_{\rm TL}=0.77\frac{v_{T_i}}{R}\sqrt{\frac{T_e}{T_i}},\quad \beta=\frac{1}{1+\ln\left(\dfrac{R^2}{r_b^2}\right)}, \tag{58}$$

where R is the radius of the cell, r_b is the laser beam radius, $\nu^{\rm rec}_{\rm TL}$ is the recombination rate in the ''free fall'' approximation of the Tonks and Langmuir theory [19], β is a correction factor for accounting the ions of interest not generating in the whole cell volume but inside the laser beam only. For helium discharge the typical electron temperature is $T_e=6-8$ eV [20]. From Eq. (58) and at $R=0.2$ cm, $r_b=0.075$ cm one can obtain

$$\nu^{\rm rec}_{\rm He_2^+}=1.8\times10^6\ \ {\rm s}^{-1}. \tag{59}$$

Only one parameter $\overline{\nu^{\rm col}}$ in Eq. (55) remains unknown. This parameter is chosen to fit the theoretical curve with the experimental data. The fitted curve is shown in Fig. 6(a) as a solid line. Note that this parameter, which is $\overline{\nu^{\rm col}_{\rm He(3^1D)}}=2.3\times10^7$ s^{-1} in our fitting, does not strongly influence the behavior of $\eta(p)$ at low pressure. This value of collision rate corresponds to the transport cross-section

$$\sigma^{\rm col}_{\rm He(3^1D)}=7.5\times10^{-15}\ \ {\rm cm}^2. \tag{60}$$

The process of the resonance exchange of excitation between $\rm He(3^1D)$ and He in the ground state slightly contributes to this collision rate because dipole transition between these states is forbidden. The inelastic collisions with excitation transfer from the state 3^1D to other sublevels of the state $n=3$ in He have cross-sections that are too small $\sim10^{-15}$ cm^2 [21] to explain the determined value (60). We suppose that the experimentally determined collision rate corresponds most likely to the elastic collision process. Indeed, considering $\rm He(3^1D)$ as hydrogenlike atom, one can estimate the radius of electron orbit as

$$r=a_0\frac{I_R}{I}, \tag{61}$$

where $a_0=0.53\times10^{-16}$ cm^2 is the Bohr radius, $I_R=13.6$ eV is Rydberg energy, and I is the ionization energy for the excited electron. For $\rm He(3^1D)$, $I=1.5$ eV and one can find $r=9a_0$. If we assume that the atom size coincides with the electron orbit radius, then the value of cross-section of elastic collision may be estimated as

$$\sigma=\pi(a_0+9a_0)^2\approx9\times10^{-15}\ \ {\rm cm}^2, \tag{62}$$

which is close to the measured value (60).

In our opinion, there is a fair quantitative agreement between the theoretical and experimental results of LIC in helium.

The behavior of experimental data for $\eta(p)$ in hydrogen discharge shows that the ionization from the state $n=3$ is caused most likely by an associative mechanism. In any case the reaction (20) is energetically admissible [ionization of H(3) due to collision with the hydrogen atom in the ground state]. However, the experimental value of the cross-section of this process is unknown; there is only information about the tentative estimations of this value $\sigma^{\rm H(3)}\leqslant10^{-16}$ cm^2 at $T=300$ K [23]. Following this estimation and accepting $\sigma^{\rm H(3)}=10^{-16}$ cm^2, one get for the associative ionization rate

$$\overline{\nu^{\rm H(3)}}=1.13\times10^6\ \ {\rm s}^{-1}\ \ {\rm torr}^{-1}, \tag{63}$$

from which it follows that, in any case, this process dominates over the rates of ionization of H(3) by electron impact or photoionization for which the previous estimations for helium are valid.

Considering $\overline{\nu^{(3)}}$ and $\overline{\nu^{\mathrm{col}}}$ as fitting parameters, we approximate the experimental data on LIC in hydrogen by the theoretical curve $\eta(p)$ (55). One can get other parameters of Eq. (55) using well-known data. At the typical temperature in hydrogen discharge $T_e = 2-3$ eV [24] Eq. (58) yields

$$\nu^{\mathrm{rec}}_{H_2^+} = 2.2\times 10^6 \ \mathrm{s}^{-1}. \tag{64}$$

The mobility of ion H_2^+ in atomic hydrogen gas is unknown for us. Therefore, we calculate the transport collision frequency of H_2^+ using the polarization potential of interaction between ion and neutral atom (hydrogen atom polarizability is $9/2a_0^3$),

$$\overline{\nu^{\mathrm{tr}}_{H_2^+}} = 3\times 10^7 \ \mathrm{s}^{-1}\ \mathrm{torr}^{-1}. \tag{65}$$

The fitted curve is shown in Fig. 6(b) as a solid line. The best agreement with experimental data is achieved at $\overline{\nu^{\mathrm{H}(3)}} = 7.5\times 10^6 \ \mathrm{s}^{-1}$ and $\overline{\nu^{\mathrm{col}}_{\mathrm{H}(3)}} = 1.15\times 10^9 \ \mathrm{s}^{-1}$.

The value of the ionization rate corresponds to the cross-section $\sigma^{\mathrm{H}(3)} = 8.6\times 10^{-16} \ \mathrm{cm}^2$, which is one order of magnitude larger than the one reported in [23]. Although our calculations do not aspire to high accuracy and have a semiquantitative nature, we suppose our estimation of the order of magnitude of the ionization cross-section of H(3) is correct. This fact indicates the noticeable divergence between our results and data from [23]. There are two possible ways to interpret the determined value of cross-section. If the main process of ionization is the reaction (20), then the cross-section value found in our experiment is one order larger than tentative theoretical estimates [23]. The second variant is the existence of some other channel of ionization, unlike (20), which may be important in our experiment and which has not been recognized.

The value of the transport collision rate $\overline{\nu^{\mathrm{col}}_{\mathrm{H}(3)}} = 1.15\times 10^9 \mathrm{s}^{-1}$ corresponds to the collision cross-section:

$$\sigma^{\mathrm{col}}_{\mathrm{H}(3)} = 1.7\times 10^{-14} \ \mathrm{cm}^2, \tag{66}$$

and this value cannot be explained by estimation (62) [for $\mathrm{H}(n=3)$, $I = 1.5$ eV and therefore the estimations (61) and (62) for elastic transport cross-section are also valid in this case].

However, there is a dipole transition between states $3P$ and $1S$ in hydrogen and, therefore, the efficiency of resonance excitation exchange between $\mathrm{H}(3P)$ and $\mathrm{H}(1S)$ may be sufficiently large. The cross-section value of this process was calculated in [25],

$$\sigma_{3P-1S} = 2.0\times 10^{-14} \ \mathrm{cm}^2. \tag{67}$$

To obtain the cross-section for resonance excitation exchange between $n=1$ and $n=3$ states of hydrogen one has to multiply Eq. (67) by the factor $g_{3P}/g_3 = 1/3$, where g_{3P} is the statistical weight of $3P$ state and g_3 is the weight of the state $n=3$ (here we assume that all sublevels of the state $n=3$ are equally populated). Then we obtain

$$\sigma_{n=3-n=1} = 0.66\times 10^{-14} \ \mathrm{cm}^2. \tag{68}$$

So, being considered separately, the processes of elastic and resonance excitation exchange collisions cannot provide the value (66). Nevertheless, we suppose that the combined action of these processes may explain this experimentally determined cross-section. For instance, assuming these processes to be independent from one another, one should sum the values (62) and (68). In this way one can obtain the estimation for collision cross-section:

$$\sigma^{\mathrm{col}}_{\mathrm{H}(3)} \approx 1.6\times 10^{-14} \ \mathrm{cm}^2. \tag{69}$$

This value is a little less than (66).

We should note here that to focus our experiment on determining the value of ionization coefficient with greater accuracy, it is better to use the cell with larger inner radius. In this case the recombination rate will decrease and the sufficiently wide interval of pressure will be available where $p\overline{\nu^{\mathrm{col}}} \ll A_{mn} + \gamma^0_m$ and $p\overline{\nu^{\mathrm{tr}}} \gg \gamma^{\mathrm{rec}}$. In this interval the dependence of $\eta(p)$ on pressure will be dropped,

$$\eta(p) = \frac{e^{-1/2}}{\sqrt{2}}\,\alpha\,\frac{ev_T}{\hbar\omega_{mn}}\,\frac{1}{\overline{\nu^{\mathrm{tr}}_i}}\,\frac{\overline{\nu^m}}{A_{mn}+\gamma^0_m}. \tag{70}$$

Eq. (70) allows one to find $\overline{\nu^m}$ with better accuracy.

IV. CONCLUSION

In this work we have presented the theory of LIC effect and the experimental results of rf discharge in helium and hydrogen. It was shown that laser radiation is capable of inducing fluxes of excited particles due to the velocity selective interaction with atoms. These fluxes transform to ion flux through ionization and, therefore, the current arises in plasma. The theoretical estimations of LIC magnitude in rf discharge in helium and hydrogen, its dependence on frequency detuning, radiation intensity, and gas pressure agree with experimental data.

We suppose that LIC may play a significant role in astrophysics. For instance, such a current may be induced in stellar atmospheres, in solar atmosphere, in particular, and may act as a source of magnetic fields. Indeed, there are sufficiently high concentrations of both neutral and ionic components of chemical elements (in addition to hydrogen) in the outer shell of stellar atmospheres. These elements provide the Fraunhofer's absorption lines in the spectrum of outgoing stellar radiation. Some absorption lines of different chemical elements may overlap producing spectral inhomegeneity of radiation for each other [26]. Thus, they are all required conditions for revealing of LIC in stellar atmospheres.

Furthermore, as we have shown in this work, the LIC experiments allow us to selectively measure the cross-section of associative ionization from excited states of different atoms. These processes play an important role in the chemical reactions of circumstellar regions [23], where there is sufficiently intense radiation to excite atoms. As a result of associative ionization the molecular ions might be produced with subsequent neutralization due to charge recombination.

ACKNOWLEDGMENTS

This work was supported by the International Science Foundation (Grant No. RCM300), the Russian Foundation of Fundamental Research and Program of Russian Universities. The authors would like to thank Dr. L.V. Il'ichev for fruitful discussion.

[1] F.Kh. Gel'mukhanov and A.M. Shalagin, Pis'ma Zh. Éksp. Teor. Fiz. **29**, 773 (1979) [JETP Lett. **29**, 711 (1979)].
[2] F.Kh. Gel'mukhanov and A.M. Shalagin, Zh. Éksp. Teor. Fiz. **77**, 461 (1979) [Sov. Phys. JETP **50**, 234 (1979)].
[3] F.Kh. Gel'mukhanov and A.M. Shalagin, Kvant. Electron. (Moscow) **8**, 590 (1981).
[4] S.G. Rautian and A.M. Shalagin, *Kinetic Problems of Nonlinear Spectroscopy* (North-Holland, Amsterdam, 1991).
[5] A.I. Parkhomenko and V.E. Prokop'ev, Opt. Spectrosc. **53**, 590 (1982).
[6] S.N. Atutov, I.M. Ermolaev, and A.M. Shalagin, Zh. Éksp. Teor. Fiz. **90**, 1963 (1986) [Sov. Phys. JETP **63**, 1149 (1986)].
[7] S.N. Atutov, K.A. Nasyrov, S.P. Pod'jachev, and A.M. Shalagin, Phys. Rev. Lett. **72**, 3654 (1994).
[8] A.I. Ferguson, Philos. Trans. R. Soc. A **307**, 645 (1982).
[9] B. Barbieri, N. Beverini, and A. Sasso, Rev. Mod. Phys. **62**, 603 (1990).
[10] J.E. Lawler, Phys. Rev. A **22**, 1025 (1980).
[11] C.V. Heer, *Statistical Mechanics, Kinetic Theory and Stochastic Processes* (Academic Press, New York, 1972).
[12] F.Kh. Gel'mukhanov, L.V. Il'ichev, and A.M. Shalagin, Physica A **137**, 502 (1986).
[13] J.J. Thomson, Philos. Mag. **23**, 412 (1912).
[14] V.R. Mironenko and A.M. Shalagin, Izv. Akad. Nauk SSSR, Ser. Fiz. **45**, 995 (1981).
[15] S.E. Frish, *Opticheskie Spektry Atomov* (Gosudarstvennoe izdatel'stvo fiziko-matematicheskoy literatury, Moscow-Leningrad, 1963).
[16] D.K. Doughty and J.E. Lawler, Phys. Rev. A **28**, 773 (1983).
[17] H.F. Wellenstein and W.W. Robertson, J. Chem. Phys. **56**, 1077 (1972).
[18] E.C. Beaty and P.L. Patterson, Phys. Rev. **137**, A346 (1965).
[19] L. Tonks and I. Langmuir, Phys. Rev. **34**, 876 (1929).
[20] R. Deloche, P. Monchicourt, M. Cheret, and F. Lambert, Phys. Rev. A **13**, 1140 (1976).
[21] H.F. Wellenstein and W.W. Robertson, J. Chem. Phys. **56**, 1072 (1972).
[22] J.R. Brandenberger, Phys. Rev. A **36**, 76 (1987).
[23] J.M. Rawlings, J.E. Drew, and M.J. Barlow, Mon. Not. R. Astron. Soc. **265**, 968 (1993).
[24] V.L. Granovskii, *Electricheskii Tok v Gase* (Nauka, Moscow, 1971).
[25] T. Watanabe, Phys. Rev. A **138**, 1573 (1965).
[26] K.A. Nasyrov and A.M. Shalagin, Astron. Astrophys. **268**, 201 (1993).